Telomere dysfunction promotes small vessel vasculitis via the LL37-NETs-dependent mechanism

Yingying Lu[1,2,3,4#], Hong Jiang[1,2,3,4#], Bingjue Li[1,2,3,4], Luxi Cao[1,2,3,4], Qixia Shen[1,2,3,4], Weiwei Yi[5], Zhenyu Ju[5], Liangliang Chen[1,2,3,4], Fei Han[1,2,3,4], Daniel Appelgren[6], Mårten Segelmark[6], Nicole de Buhr[7,8], Maren von Köckritz-Blickwede[7,8], Jianghua Chen[1,2,3,4]

[1]Kidney Disease Center, The First Affiliated Hospital, College of Medicine, Zhejiang University, Hangzhou 310003, China; [2]Kidney Disease Immunology Laboratory, The Third Grade Laboratory, State Administration of Traditional Chinese Medicine of PR China, Hangzhou 310003, China; [3]Key Laboratory of Multiple Organ Transplantation, Ministry of Health, Hangzhou 310003, China; [4]Key Laboratory of Nephropathy, Hangzhou 310003, China; [5]Institute of Aging Research and Max-Planck-Research Group on Stem Cell Aging, Hangzhou Normal University, Hangzhou 311121, China; [6]Department of Medical and Health Sciences (IMH), Linkoping University, Linkoping, Sweden; [7]Department of Physiological Chemistry, University of Veterinary Medicine Hannover, Hannover, Germany; [8]Department of Physiological Chemistry and Research Center for Emerging Infections and Zoonoses (RIZ), University of Veterinary Medicine Hannover, Hannover, Germany

Contributions: (I) Conception and design: H Jiang , J Chen; (II) Administrative support: J Chen, Z Ju, M Segelmark, MV Köckritz-Blickwede; (III) Provision of study materials or patients: L Chen, F Han; (IV) Collection and assembly of data: Y Lu, H Jiang, B Li, L Cao, Q Shen, W Yi, D Appelgren, ND Buhr, MV Köckritz-Blickwede; (V) Data analysis and interpretation: Y Lu, H Jiang; (VI) Manuscript writing: All authors; (VII) Final approval of manuscript: All authors.

[#]These authors contributed equally to this work.

Correspondence to: Professor Hong Jiang, PhD; Professor Jianghua Chen, MD. Kidney Disease Center, The First Affiliated Hospital, School of Medicine, Zhejiang University, Hangzhou 310003, China. Email: annie.jh@163.com; chenjianghua@zju.edu.cn.

Background: Small vessel vasculitis (SVV) is a group of systemic autoimmune diseases that are mediated by neutrophil extracellular traps (NETs) in response to cathelicidin LL37, an aging molecular marker, which could be induced by telomere dysfunction. Therefore, in this study, we evaluated the hypothesis that telomere dysfunction in neutrophils may promote SVV via an LL37-NETs-dependent mechanism.

Methods: We contrasted the release of neutrophil NETs from mice with telomere dysfunction, mice with DNA damage and wide-type mice. Neutrophil telomere length, the expression of LL37, and the formation of NETs were measured in SVV patients and healthy controls (HCs). The co-expression of γH2AX, LL37, and NETs were detected in SVV patients to evaluate the association of the immune aging of neutrophils and pro-inflammatory conditions. LL37 inhibitor was used to verify its key role in NETs release in SVV patients and DNA damage mice.

Results: We found that NETs were over-induced by telomere dysfunction and DNA damage in mice, which may be associated with a marked increase in LL37. For patients with SVV, telomeres in neutrophils were significantly shortened, which was also associated with higher levels of LL37 and NETs. Inhibition of LL37 reduced the NETs released from neutrophils.

Conclusions: Taken together, the results of these studies suggest that dysfunction of telomeres may promote SVV through the mechanism of LL37-dependent NETs. Thus, targeting the LL37-NETs may be a novel therapy for SVV.

Keywords: Telomere dysfunction; DNA damage; small vessel vasculitis (SVV); LL37; neutrophil extracellular traps (NETs)

Introduction

Small vessel vasculitis (SVV) is a group of systemic autoimmune diseases that are characterized by necrotizing inflammation within the vessel wall and the presence of anti-neutrophil cytoplasmic autoantibody (ANCA) (1). This happens mostly in the elderly, with a peak age of 65 to 74 years (2). When the kidney is involved, it manifests as pauci-immune necrotizing and crescentic glomerulonephritis pathophysiologically (2). Neutrophils play a key role in the pathogenic process since they infiltrate the renal interstitium, necrotizing capillary loops, and the crescent of glomerulus during the acute stage. These are both effector cells and autoimmune vectors for the disease (3,4).

Recent studies implicated the role of neutrophil extracellular traps (NETs) in breaking immune tolerance and promoting organ damage in SVV (5,6). NETs are characterized by the presence of neutrophil nuclear DNA fibers in the extracellular space. Histones and antimicrobial proteins such as myeloperoxidase (MPO), proteinase-3 (PR3), and human cathelicidin LL37 reside on them (7). Previous studies found that neutrophils activated by ANCA produced NETs and released LL37 *in vitro* (8). There was also evidence for NETs formation and LL37 deposition in kidney tissue in individuals with SVV (8). Interestingly, in 2014, Neumann *et al.* found the role of LL37 in facilitating the formation and stabilization of the structure of NETs (9,10). The interaction of LL37 and NETs may be a new mechanism for SVV.

We reported a group of biomarkers for aging induced by telomere dysfunction and DNA damage in 2008 (11). These markers were not only highly expressed in old, fourth generations of telomerase knockout mice (G4 mTerc$^{-/-}$) but were also increasingly expressed during human aging and in telomere-dysfunction-related diseases, such as cirrhosis and myelodysplastic syndromes (MDS) (11).

LL37 related to NETs seems pathogenic for SVV. However, whether LL37 induced by telomere-dysfunction has a role in regulating NETs in SVV is still unknown.

Hence, we proposed that the pathological immune senescence of aging neutrophils will negatively affect their activity due to DNA damage and telomere dysfunction. As a result, it would develop more LL37 and interfere with NETs, ultimately leading to renal damage and SVV progression.

Methods

Animals

Terc$^{+/-}$ mice were provided by the Institute of Aging Research and Max-Planck-Research Group on Stem Cell Aging, Hangzhou Normal University. In order to obtain the fourth generation of telomerase knockout (G4mTerc$^{-/-}$) mice with severe telomere dysfunction, Terc$^{+/-}$ mice were intercrossed to produce Terc$^{-/-}$ mice, and then Terc$^{-/-}$ mice were intercrossed successively to decrease telomere reserves in the pathogen-free animal facility of Zhejiang University. All mice were of a C57BL/6J background. The experiments were approved by our institution's Ethics Committee for Investigation with Animals.

The isolation of neutrophils and irradiation procedures used

Murine neutrophils were isolated from bone marrow, as previously described (10). Briefly, bone marrow cells were flushed from the femur and tibia with RPMI-1640 (life technologies) +2% Fetal Bovine Serum (FBS, Life technologies). After filtration through a cell strainer (100 μm; BD Falcon, San Jose, CA, USA) and erythrocyte lysis with sterile water, the cells were incubated for 1 h at 37 ℃ with 5% CO_2 to separate the suspended granulocytes from adherent monocytes.

PolymorphPrep^{TM} (Progen Biotechnik) was used according to the manufacturer's instructions, as previously described (9), to isolate human neutrophils from fresh blood.

For the irradiation assay, neutrophils were irradiated with a dose of 10 Gy using an RS-2000 X-Ray Biological Irradiator (Rad Source Technologies) after being seeded onto 24-well plates.

Visualization of NETs formed in vitro

In vitro, NETs were visualized as previously described (9,10). Briefly, a total of 5×10^5 neutrophils/well were seeded in 24-well plates and cultivated in the presence or absence of 40 μg/mL aprotinin (A1153 Sigma) at 37 ℃ in 5% CO_2 for 3 hours. After fixation, permeabilization, and blocking, cells were incubated with mouse anti-DNA/histone 1 monoclonal antibody (MAB 38624, Millipore, USA), followed by Alexa-Fluor-488-labeled goat-anti-mouse

Table 1 The characteristics of human samples

Characteristics	SVV (n=70)	HCs (n=70)	P value
Gender, male/female, n/n	45/25	45/25	1
Age, mean ± SD, year	56.46±13.51	56.40±5.17	0.9737
WBC, mean ± SD, n×10^9	7.85±3.43	5.62±1.72	<0.0001
ANCA at diagnosis, PR3-ANCA/MPO-ANCA/ANCA negative, n	63/4/3	NA	NA
Serum creatinine, medium (IQR), µmol/L	274.5 (152.25–507.25)	56 (50.25–58)	<0.0001
Estimated GFR, medium (IQR), mL/minute/1.73 m^2	20 (9.025–36.70)	109.675 (96.59–121.54)	<0.0001
Urinary protein, mean ± SD, g/24 hours	2.34±1.647	NA	NA

WBC, white blood cell count; IQR, interquartile range; eGFR, estimated glomerular filtration rate; NA, not available.

antibody (Life Technologies). Slides were mounted, and images were randomly acquired using confocal fluorescence microscopy installed with a Leica TCS SP8 microscope with an HCX PL APO CS2 63× oil immersion objective. Control preparations treated with an isotype antibody was used to adjust the settings. For each preparation, a minimum of five random images from three independent subjects was acquired. Data were expressed as percentages of NET-producing neutrophils.

Subjects

The study protocols followed the Declaration of Helsinki. SVV was diagnosed according to the Chapel Hill Consensus Conference (CHC) definitions (12). SVV patients with renal involvement (n=70) and kidney transplantation donors, namely healthy controls (HCs, n=70), were recruited from our hospital with written consent. There was no significant difference in the age between the two groups (56.46±1.615 *vs.* 56.40±0.6173, P=0.9737). The ratio of males and females was the same between the two groups (male/female =25/45), thereby avoiding the potential effects of sexual differences. The sample characteristics are presented in *Table 1*. Blood samples and specimens from renal needle biopsies were obtained and used anonymously.

Real-time polymerase chain reaction (RT-PCR)

We used RT-PCR to determine the telomere length of human neutrophils. Firstly, genomic DNA (Axygen, USA) was extracted from human neutrophils, and the telomere length of a set of standard cell lines was assessed by Southern blotting. Then, RT-PCR was carried as previously described (13). Briefly, Telomere (T) PCR and

single-copy gene human β-globin (S) PCR were conducted. The reactions were performed on a Prism7500 (Applied Biosystems), and data were collected and analyzed using ABI Prism7500 SDS v.1.7 software.

Indirect Enzyme-Linked Immunosorbent Assay (ELISA) of LL37

After coating the microwell plates (NUNC) with 50 µL serum, we applied a 1% milk-Phosphate Buffered Saline (PBS) solution to block the added binding sites on the plastic surface. Then, the plates were incubated with the primary antibody, mouse-anti-human LL-37 (Hycult biotech, The Netherlands) 1:500 (v/v) and horseradish peroxidase (HRP)-hapten conjugated secondary antibody (DW0990, Dawen Biotec, USA) 1:2,000 (v/v) at room temperature for 2 h. After each step, the plates were washed three times with PBST wash solution (PBS with 0.05% Tween 20) to remove the unattached material. Each well was then incubated with 100 µL tetramethyl benzidine peroxide-based substrate solution for 15 min. The color reaction was stopped with 20 µL/well 2 M H_2SO_4 stop solution. Absorbances were at once read in the microplate reader at 450 nm (ELX800NB BioTek USA).

Cell-free (cf)-DNA

To quantify levels of free DNA released into circulation in human serum samples, the Quant-iT Pico Green double-stranded DNA (dsDNA) assay was conducted according to the manufacturer's instructions (Invitrogen, Germany). It is based on an ultrasensitive fluorescent nucleic acid stain of dsDNA in solution. The serum samples were diluted 10-fold with TE buffer (10 mM Tris-HCl, 1 mM EDTA,

pH 7.5) before detection. A standard calibration curve was acquired using a lambda DNA standard in all analyses. The fluorescence intensity was measured with a fluorescence microplate reader (excitation at 480 nm wavelength, emission at 520 nm wavelength, infinite M200, TECAN) and quantified using Magellan V6.1 software.

NETs remnant ELISA

NETs remnant ELISA was conducted as previously described (14). Briefly, after coating 96-well microplates with a monoclonal mouse anti-nucleosome antibody (B6. SLE-1, 0.5 mg/mL) and blocking the additional binding sites, the plates were incubated with standards and serum for 2 h at room temperature. A rabbit anti-human MPO (1:500; DAKO, Carpinteria, CA, USA) was then added for 1 h at room temperature and an alkaline phosphatase-conjugated swine anti-rabbit antibody (1:500, DAKO) for another hour. Finally, a substrate for alkaline phosphatase (4-nitrophenyl phosphate disodium salt hexahydrate; Sigma-Aldrich, St Louis, MO, USA) was added, and the plates were read at 405 nm using a VersaMax ELISA microplate reader (Molecular Devices, Sunnyvale, CA, USA). A standard curve was constructed for each plate, and all samples were interpolated from it.

Immunofluorescent staining of in situ NETs

Immunofluorescent staining was performed on frozen sections of kidney needle biopsies to obtain *in situ* evidence of NET formation. After permeabilization with 0.2% Triton X-100 and blocking with 1.5% goat serum, slides were incubated with a monoclonal antibody, mouse anti-DNA/histone 1 (MAB 38624, Millipore, USA), followed by a secondary antibody, Alexa-Fluor-488-labeled goat-anti-mouse antibody (Life Technologies). For the co-localization assay of NETs and LL37, rabbit-anti-human LL-37 and Alexa-Fluor-594-labeled goat-anti-rabbit antibody were co-incubated with the corresponding antibody. Slides were mounted in ProlongGold® antifade with DAPI (136933; Invitrogen) and viewed using confocal fluorescence microscopy with a Leica TCS SP5 microscope with an HCX PL APO 40x oil immersion objective.

Telomere, rH2AX, and LL37 triple-staining

Briefly, after paraffin-embedded sections from kidney needle biopsies were dewaxed and the antigens were retrieved, the slides were incubated in acidified pepsin (Sigma Aldrich, USA) and dehydrated through graded alcohols. A FITC-labeled PNA probe specific for (TTAGGG)n sequences (PANAGENE, Korea) was co-denatured with the slide at 80 ℃ for 3 min and hybridized at RT for 2 h. Slides were then incubated first with the mouse-anti-human LL37 (HM2070, Hycult biotech, The Netherlands) and rabbit-anti-γH2AX (MABE205, Millipore, USA) antibodies, followed by the secondary Alexa-Fluor-594-labeled goat-anti-mouse antibody and Alexa-Fluor-488-labeled goat-anti-rabbit antibody. Slides were mounted ProlongGold® antifade with DAPI (Invitrogen, Paisley, UK) and finally visualized with confocal fluorescence microscopy using a Leica TCS SP8 microscope with an HCX PL APO CS2 63× oil immersion objective.

Statistical analyses

Statistical analyses were performed using the MedCalc software package (MedCalc for Windows 8.1.1.0, MedCalc Software), SPSS16 .0, (SPSS, Inc., Chicago, IL, USA) and GraphPad Prism 5 (San Diego, CA, USA). A one-sample Kolmogorov-Smirnov test was performed to evaluate the normal distribution of data. The unpaired Student's *t*-test or Mann-Whitney test was used for the assessment of statistical significance between two groups with continuous variables. The results are presented as the mean ± SEM or the mean ± SD or the median (interquartile range). The error bars are present in all figures. Data were considered statistically significant at P<0.05.

Results

NETs are over-induced in response to telomere dysfunction and DNA damage in mice

The fourth generation of telomerase knockout (G4mTerc$^{-/-}$) mice exhibited aging condition when they were 12 months old, while wide type mice (WT) did not start until 24 months old (15). So, we identified NETs released by the neutrophils from 12-month-old G4mTerc$^{-/-}$ mice (as a premature aging group), 12-month-old WT (as same-age control), and 24-month-old WT (as same aging condition control). The percentage of netting neutrophils increased in 12-month-old G4mTerc$^{-/-}$ mice compared to 12-month-old WT (mean ± SEM: 24.69%±2.32% *vs.* 12.06%±0.72%, P<0.0001, *Figure 1A*) or 24-month-old WT (mean ± SEM:
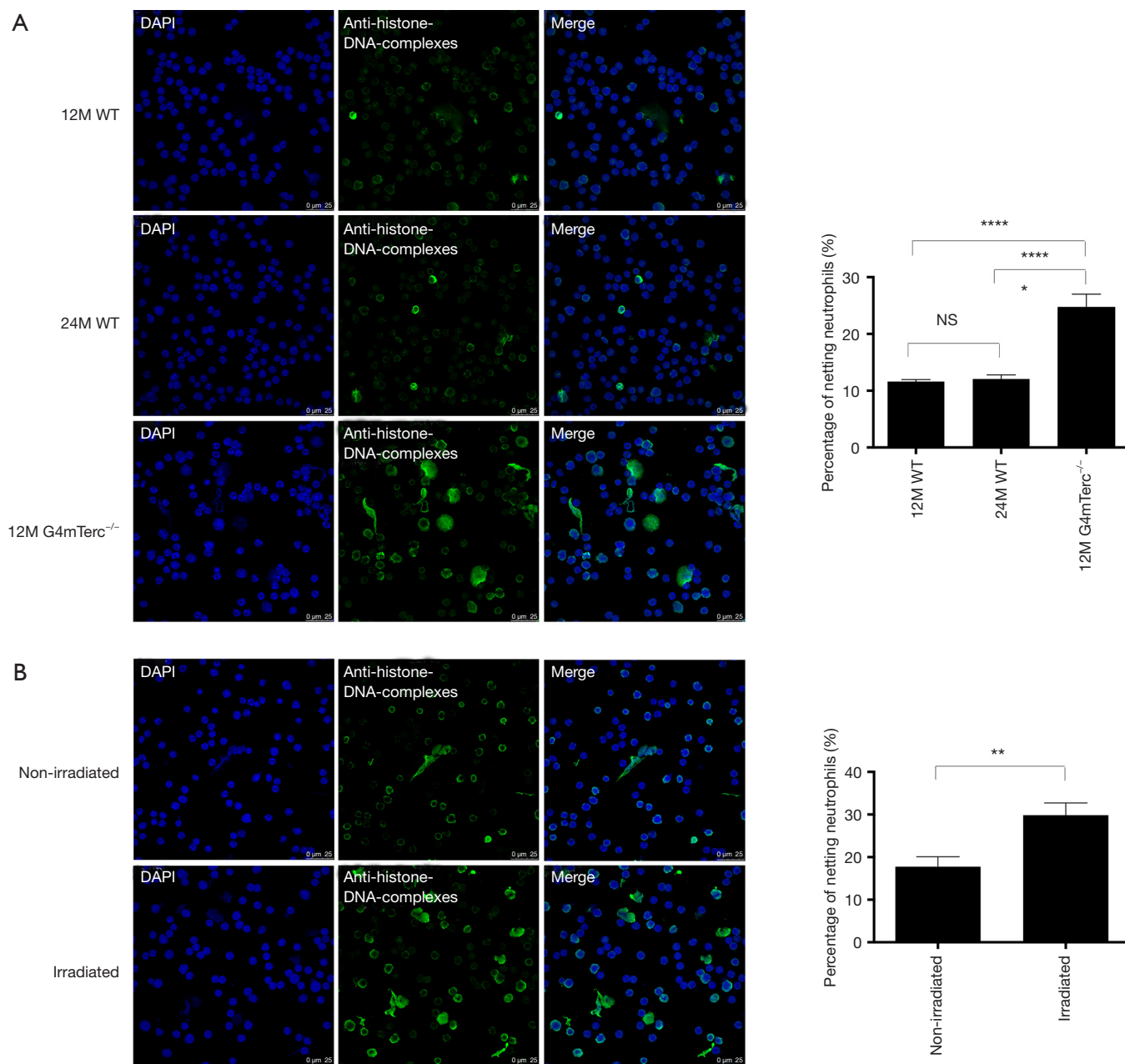
Figure 1 Mice neutrophils produce more NETs in response to telomere dysfunction or DNA damage. (A) The percentage of netting neutrophils from the 12-month-old fourth generations of telomerase knockout mice (G4mTerc⁻/⁻) and wide type mice of different ages (WT); (B) the netting rate of irradiated and non-irradiated neutrophils from 2-month-old WT mice. The graph is a minimum of 15 images derived from 3 independent experiments. The error bars of the graph represent SEM. Unpaired Student's *t*-test was conducted to analyze the statistical significance of two independent experiments. ****, P<0.0001; **, P<0.01, NS, not significant; 2M, 2-month-old; 12M, 12-month-old; 24M, 24-month-old.

24.69%±2.32% *vs.* 11.61%±0.35%, P=0.0131, *Figure 1A*). NET release rate was similar in WT of different ages (mean ± SEM, 12-month-old WT *vs.* 24-month-old WT:

12.06%±0.72% *vs.* 11.61%±0.35%; P=0.5907, *Figure 1A*).

Irradiation assay was conducted to the neutrophils of 2-month-old WT to build a model of DNA damage.

Compared to non-irradiated neutrophils, irradiated neutrophils that suffered DNA damage tended to form more NETs (mean ± SEM: 29.86%±2.85% *vs.* 17.76%±2.33%, P=0.0027, *Figure 1B*).

Neutrophils from SVV patients have shortened telomeres and produce higher levels of LL37 and NETs in vivo

We used real-time polymerase chain reaction to detect the telomere lengths of neutrophils from SVV patients and HCs. The telomeres of neutrophils from SVV patients were significantly shortened compared to those from healthy individuals (mean ± SEM: 8.35±0.24 *vs.* 11.32±0.26, P<0.0001, *Figure 2A*).

The relative concentration of LL37 was measured using enzyme-linked immunosorbent assay (ELISA). The results were expressed as the optical density value. We found significantly increased serum LL37 levels in patients with SVV compared to HCs (mean ± SEM: 1.229±0.024 *vs.* 0.954±0.014 a.u., P<0.0001, *Figure 2B*). The concentration of urine LL37 was low in both groups. However, urine LL37 levels in patients with SVV remained higher than in HCs (mean ± SEM: 0.032±0.005 *vs.* 0.009±0.001 a.u., P<0.0001, *Figure 2C*).

We quantified NETs in circulation by evaluating the levels of major NET components, a NET remnant (nucleosome-MPO complexes), and cell-free DNA (cf-DNA).

Increased levels of NET remnants were found in patients with SVV compared to HCs (mean ± SEM: 252.6±25.83 *vs.* 184.3±12.61 a.u., P=0.0189) (*Figure 2D*). Patients with SVV also showed higher cf-DNA levels compared with healthy individuals (mean ± SEM: 393.9±19.78 *vs.* 269.2±8.552 ng/mL; P<0.0001, *Figure 2E*).

Immunofluorescent staining showed that NETs were deposited in the kidney tissue of SVV patients, while no NET deposition was found in HCs (*Figure 2F*). Furthermore, *in situ*, NETs were decorated with the immunostimulatory peptide LL37 (*Figure 2G*).

Aging neutrophils with telomere shortening and DNA damage produce LL37 and NETs in the renal injury of SVV patients

To evaluate the association of the immune aging of neutrophils and pro-inflammatory conditions, we conducted telomere-γH2AX, a double-stranded DNA damage marker, and LL37 triple-staining (*Figure 3A*). As shown in *Figure 3A*,

neutrophils, characterized by containing a polymorphic nucleus, infiltrated the kidney tissue of SVV patients. In these polymorphic nuclei, the staining of γH2AX was co-localized to telomere staining, which showed telomere damage. During this time, LL37 assembled at the nuclear periphery. We also captured a field of LL37 surrounding a polymorphic nucleus in the background of NET deposition in the kidney tissue of SVV patients (*Figure 3B*). These results show that the immune aging of neutrophils and inflammatory medium release co-exist in SVV patients. And LL37 may build a bridge between telomere dysfunction and NETs production of neutrophils.

### Neutrophils from SVV produce more NETs in vitro, and LL37 mediates this process

To investigate whether neutrophils from SVV were more active in the circulation, we evaluated the ability for NET production by neutrophils from HCs and SVV patients in vitro. As shown in *Figure 4A*, Neutrophils from SVV patients produced more NETs than those from HCs (mean ± SEM: 54.66%±5.12% *vs.* 33.18%±2.70%, P=0.0002, *Figure 4A*).

We also conducted an irradiation assay to induce DNA damage in neutrophils from healthy donors. Irradiated human neutrophils tended to produce more NETs compared to non-irradiated human neutrophils (mean ± SEM: 47.48%±2.77% *vs.* 33.18%±2.70%, P=0.0018, *Figure 4A*). There was no significant difference in NET production ability between SVV neutrophils or irradiated neutrophils (P=0.2276, *Figure 4A*).

Interestingly, when SVV neutrophils were treated with aprotinin, a serine protease inhibitor, to competitively block the activation of endogenous LL-37 (16), a significantly lower degree of NET formation was detectable (mean ± SEM: 29.79%±3.92% *vs.* 50.25%±4.71%, P=0.0024, *Figure 4B*). However, aprotinin did not affect the NET release of neutrophils from healthy subjects (mean ± SEM: 29.59%±4.03% *vs.* 30.74%±3.77%, P=0.8354, *Figure 4B*). Similarly, the NET release process during irradiation was also suppressed by aprotinin (mean ± SEM: 42.38%±4.652% *vs.* 27.85%±3.651%, P=0.0205, *Figure 4C*).

Discussion

Here, we found the novel regulatory mechanisms of aging neutrophils through LL37-NETs interactions to promote SVV, supplying basic and clinical implications.
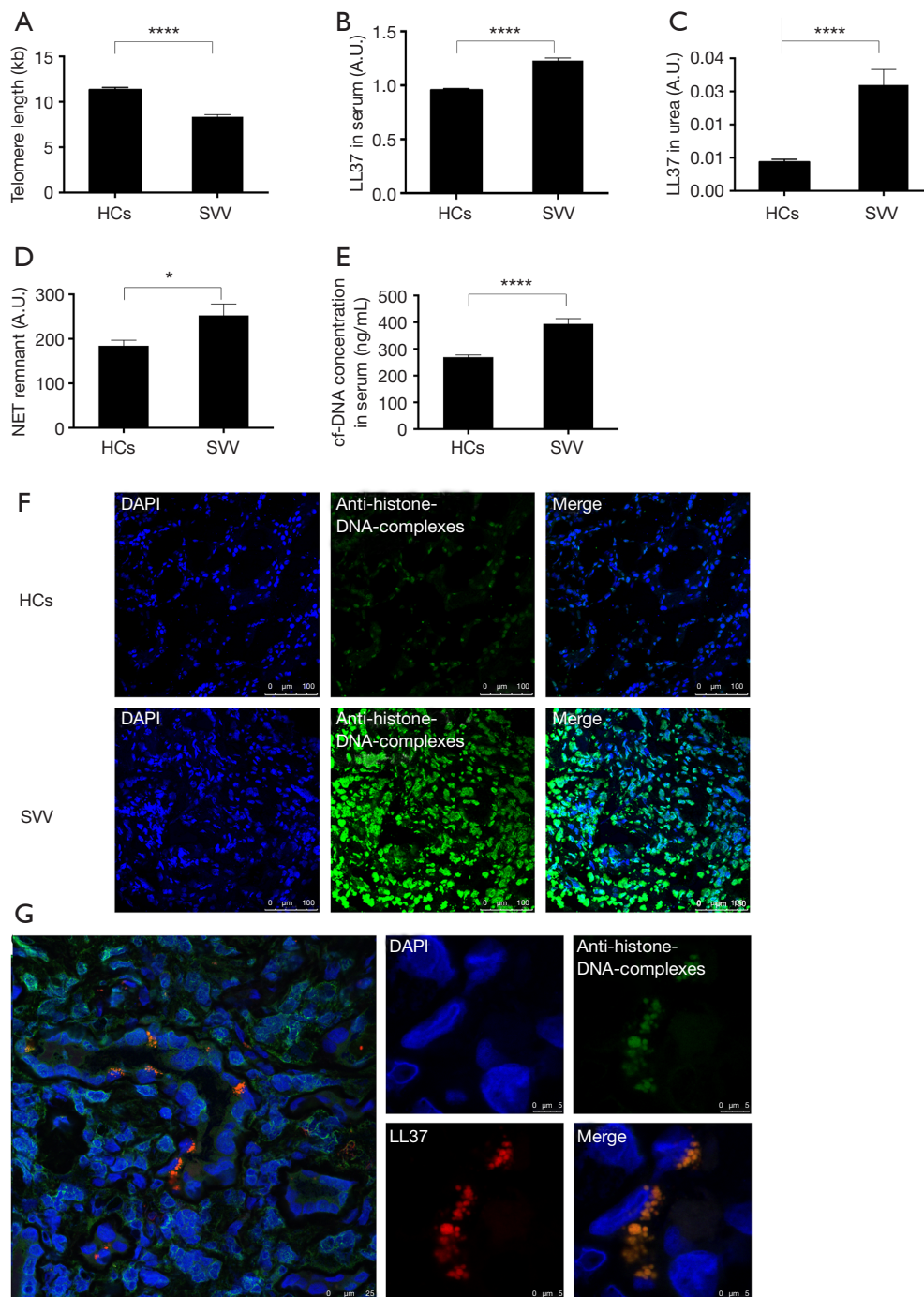
Figure 2 Higher levels of LL37 expression and NET release are determined in patients with SVV. (A) Telomere length of SVV and HCs by real-time Q-PCR; (B) levels of LL37 in serum from the disease group and healthy group; (C) levels of LL37 in urine from the disease group and healthy group; (D) levels of NET remnants in serum from patients with SVV or HCs; (E) levels of cf-DNA in serum from patients with SVV or HCs (A-E). N=70 for each group. The error bars of the graph represent the SEM. Unpaired Student's *t*-test was conducted to analyze the statistical significance of two independent experiments; (F) an Alexa 488-labeled antibody against H2A-H2B-DNA complexes was used to visualize NETs in green, and DAPI was used to stain the nuclei in blue. Pictures were merged to form an overlay image; (G) H2A-H2B-DNA complexes, LL37, and nuclei are stained green, red, and blue, respectively. Pictures were merged to form an overlay image. A.U., arbitrary unit.
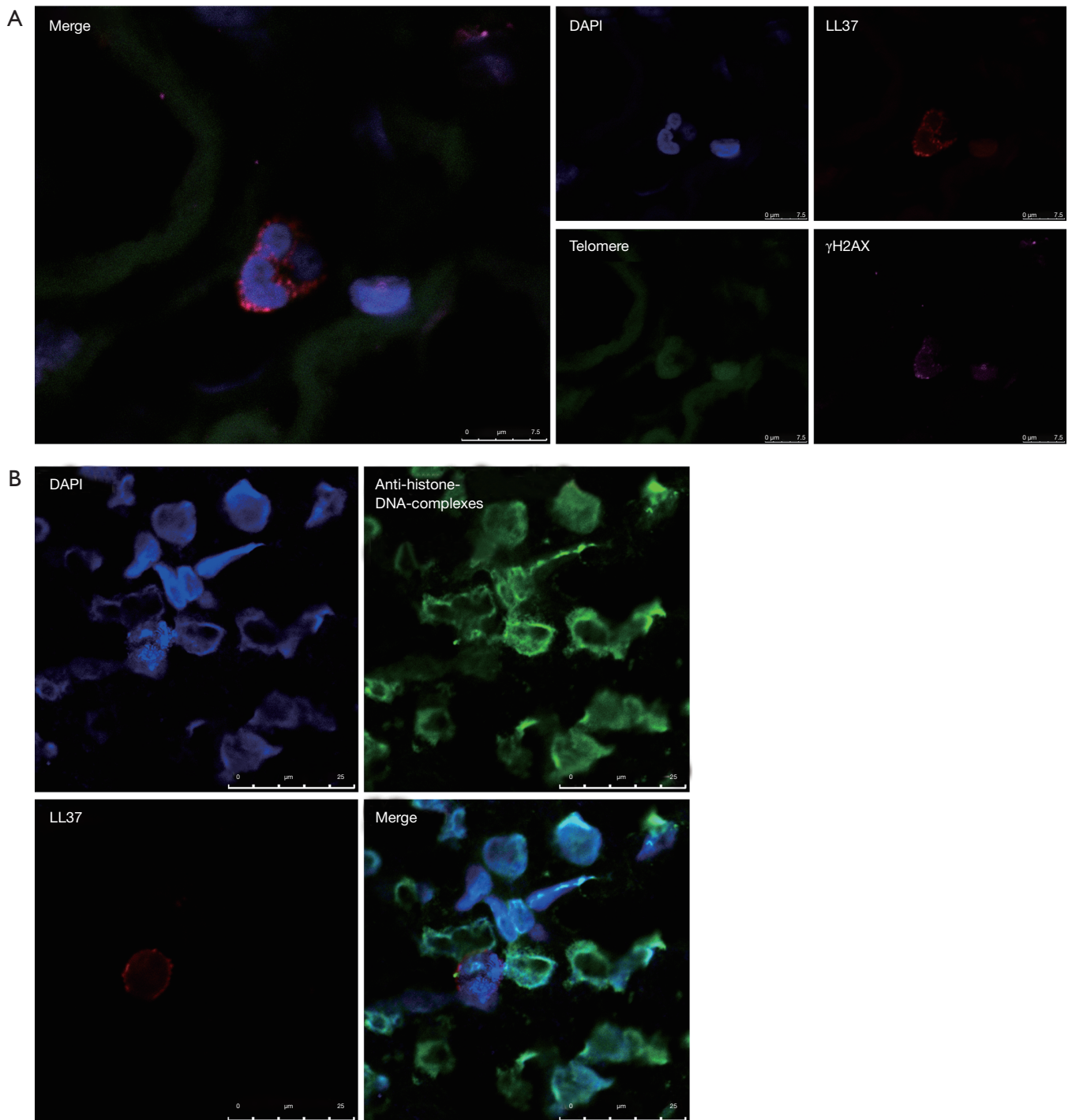
Figure 3 Immune aging of neutrophils and inflammatory medium release are determined *in situ* in individuals with SVV. (A) Neutrophils (polymorphic nuclear) infiltrated the kidney tissue from patients with SVV. Telomere dysfunction was found by the co-localization of γH2AX (purple) and telomeres (green) in the nucleus (DNA in blue). Immunostaining of LL37 showed perinuclear LL37 (red) in neutrophils that suffered DNA dysfunction; (B) H2A-H2B-DNA complexes, LL37, and nuclei are stained green, red, and blue, respectively. Pictures were merged to form an overlay image. LL37 assembled around the polymorphic nucleus in a background of NET deposition in the kidney tissue of SVV patients.
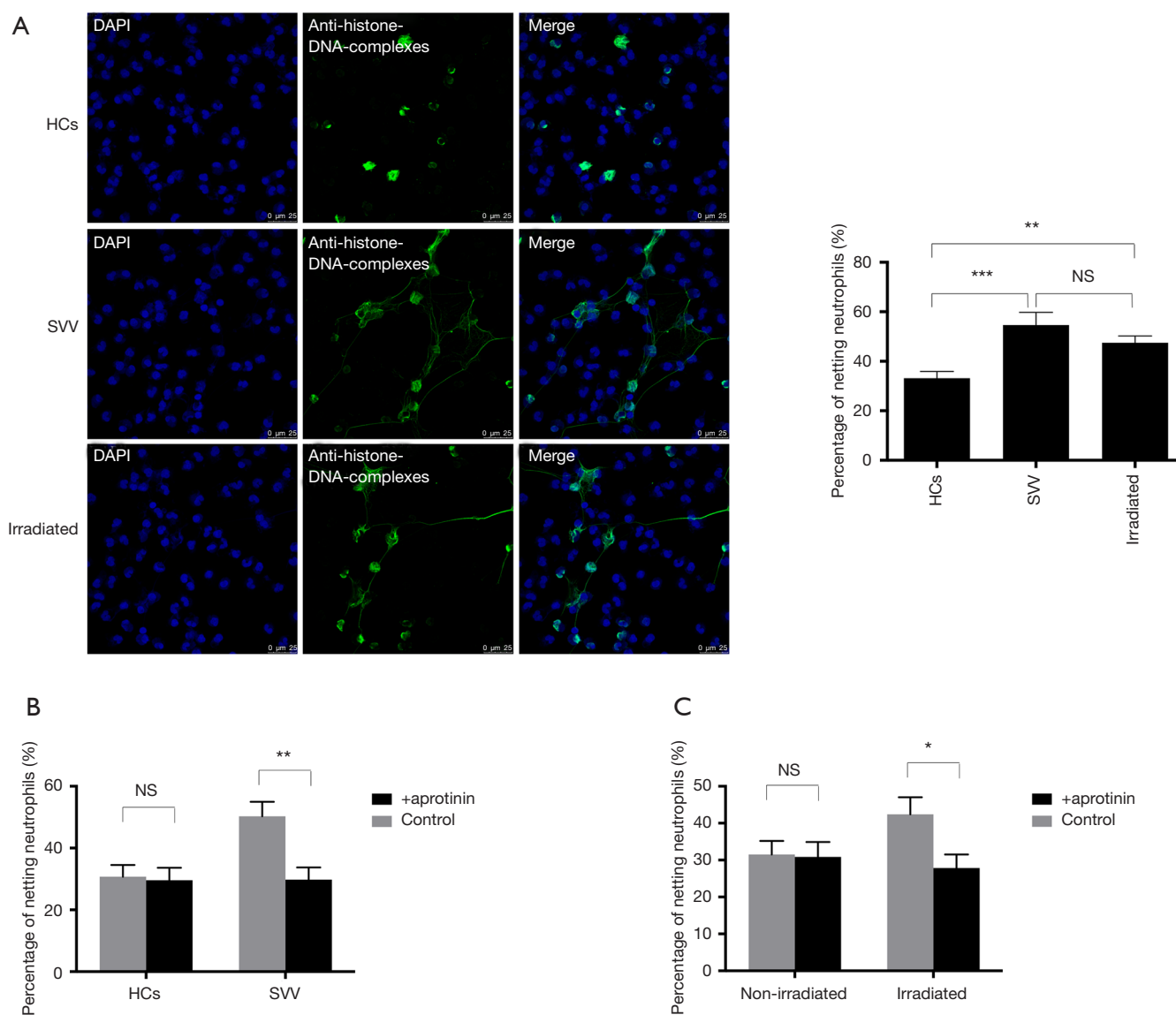
Figure 4 Human neutrophils from SVV produce more LL37-mediated-NETs. (A) The percentage of spontaneously netting neutrophils from healthy controls (HCs) and SVV patients and the percentage of netting neutrophils after irradiation; (B) degree of NET release of neutrophils from HCs and SVV in the presence or absence of aprotinin; (C) degree of NET release of neutrophils after irradiation in the presence or absence of aprotinin. The graph is a minimum of 15 images derived from 3 independent experiments. The error bars of the graph represent SEM. Unpaired Student's *t*-test was conducted to analyze the statistical significance of two independent experiments. ***, P<0.001; **, P<0.01; *, P<0.05; NS, not significant.

Increasingly evidence proves that NETs have a key role in tissue injury and dysfunction in systemic autoimmunity. The mechanism of how NETs affect end-organ tissues in SVV was well investigated, including interaction with myeloid dendritic cells (17) or endothelial cells (18), alternative complement pathway activation (19), and thrombin generation (20). However, the mechanisms mediating NET release need a better understanding. The present study supplies evidence for the first time depicting the NET response to telomere dysfunction and DNA damage (*Figure 1A,B*). Interestingly, NETs were not associated with the normal aging of WT (*Figure 1A*). The

observation that mouse telomeres had not shortened enough to show phenotypic changes during normal aging could partly explain this. Zhang *et al.* found aged neutrophils with high expression of CXCR4 and low expression of CD62L release excessive NETs, which strengthened our results that senescent neutrophils are overly-activated in circulation (21).

Earlier studies found that telomere-driven premature senescence showed in individuals with chronic activation of the immune system. Accelerated telomere loss was implicated in different leukocyte subpopulations as a common feature of autoimmune diseases (22-24). These studies mainly focused on monocyte and lymphocyte subpopulations (25-28). Evidence for telomere shortening of T cells derived from patients with GPA, a subtype of SVV, was provided (29). The telomere erosion of neutrophils was discovered previously in SLE, however (30).

In the present study, we discovered for the first time that telomere erosion existed in neutrophils from individuals with SVV, with evidence of telomere shortening in neutrophils in circulation (*Figure 2A*) and DNA damage foci at dysfunctional telomeres in neutrophils infiltrating the renal tissue (*Figure 2F*). An increased renewal and replicative senescence due to chronic inflammation may accelerate telomere loss of leukocytes (31). Another factor may be the increased oxidative stress and oxidative DNA damage that cause telomere erosion, which has already been found in another autoimmune disease (32,33).

Our earlier study showed that cramp, the homologous peptide of LL37 in mice, is a biomarker of aging and telomere dysfunction. Cramp was overexpressed in late generations of telomerase knockout mice (G4mTerc$^{-/-}$) and up-regulated in response to DNA damage after irradiation (11). Additionally, LL37 is a major component of NETs (31). After release by neutrophils, LL37 can interact with NETs and protect NETs from degradation by nucleases (9). Our present study speculated that LL37 might be associated with NETs release by aging neutrophils in SVV since the increased level of LL37 and NETs was identified in serum (*Figure 2B,D,E*) and kidney tissue (*Figure 2F,G*) from SVV patients. Zhang *et al.* strengthened our results, whose data suggested that higher levels of LL-37 were observed in SVV patients, particularly those with crescentic formation (8).

Interestingly, we also found that LL37 surrounded the nucleus of neutrophils that suffered telomere dysfunction (*Figure 3A*) and produced a significant amount of NETs (*Figure 3B*) in the kidney tissue of SVV patients. This shows

that LL37 may function as a bridge between telomere dysfunction and NET production of neutrophils. This may occur because neutrophils suffering from telomere dysfunction or DNA damage produce more LL37 (11). In our present study, we also found that inhibition of LL37 reduced the NETs released by neutrophils from SVV or after irradiation (*Figure 4B,C*). Telomere dysfunction taken together may promote SVV via the LL37-dependent NETs mechanism.

In conclusion, our study shows that the immune aging of neutrophils induced by DNA damage and telomere dysfunction could result in the over-release of NETs and the high expression of LL37. Consequently, NETs were deposited in the kidney tissue and caused persistent damage, finally affecting SVV disease progression. Notably, this study could not clarify the exact mechanism of LL37 regulation driven by telomere dysfunction. Further studies are needed to elucidate this process. Because many immune-mediated pathologies share common immunological mechanisms biomarkers for SVV and other chronic inflammatory diseases that theoretically may be LL37 or NETs. Therefore, they may be established as antagonists in future therapies. Because many immune-mediated pathologies share common immunological mechanisms, LL37 or NETs may potentially be biomarkers for SVV and other chronic inflammatory diseases. Furthermore, their antagonists could be developed as potential therapies.

Footnote

Conflicts of Interest: The authors have no conflicts of interest to declare.

Ethical Statement: The authors are accountable for all aspects of the work in ensuring that questions related to the accuracy or integrity of any part of the work are appropriately investigated and resolved. The local Ethics Committee approved the study of the First Affiliated

Hospital, School of Medicine, Zhejiang University (2016-354), and written informed consent was obtained from all patients.

References

1. Nakazawa D, Masuda S, Tomaru U, et al. Pathogenesis and therapeutic interventions for ANCA-associated vasculitis. Nat Rev Rheumatol 2019;15:91-101.
2. Geetha D, Jefferson JA. ANCA-Associated Vasculitis: Core Curriculum 2020. Am J Kidney Dis 2020;75:124-37.
3. Thieblemont N, Wright HL, Edwards SW, et al. Human neutrophils in auto-immunity. Semin Immunol 2016;28:159-73.
4. Schreiber A, Choi M. The role of neutrophils in causing antineutrophil cytoplasmic autoantibody-associated vasculitis. Curr Opin Hematol 2015;22:60-6.
5. Frangou E, Vassilopoulos D, Boletis J, et al. An emerging role of neutrophils and NETosis in chronic inflammation and fibrosis in systemic lupus erythematosus (SLE) and ANCA-associated vasculitides (AAV): Implications for the pathogenesis and treatment. Autoimmun Rev 2019;18:751-60.
6. Gupta S, Kaplan MJ. The role of neutrophils and NETosis in autoimmune and renal diseases. Nat Rev Nephrol 2016;12:402-13.
7. Papayannopoulos V. Neutrophil extracellular traps in immunity and disease. Nat Rev Immunol 2018;18:134-47.
8. Zhang Y, Shi W, Tang S, et al. The influence of cathelicidin LL37 in human anti-neutrophils cytoplasmic antibody (ANCA)-associated vasculitis. Arthritis Res Ther 2013;15:R161.
9. Neumann A, Vollger L, Berends ET, et al. Novel role of the antimicrobial peptide LL-37 in the protection of neutrophil extracellular traps against degradation by bacterial nucleases. J Innate Immun 2014;6:860-8.
10. Neumann A, Berends ET, Nerlich A, et al. The antimicrobial peptide LL-37 facilitates the formation of neutrophil extracellular traps. Biochem J 2014;464:3-11.
11. Jiang H, Schiffer E, Song Z, et al. Proteins induced by telomere dysfunction and DNA damage represent biomarkers of human aging and disease. Proc Natl Acad Sci U S A 2008;105:11299-304.
12. Jennette JC, Falk RJ, Bacon PA, et al. 2012 revised International Chapel Hill Consensus Conference Nomenclature of Vasculitides. Arthritis Rheum 2013;65:1-11.
13. Cawthon RM. Telomere measurement by quantitative PCR. Nucleic Acids Res 2002;30:e47.
14. Söderberg D, Kurz T, Motamedi A, et al. Increased levels of neutrophil extracellular trap remnants in the circulation of patients with small vessel vasculitis, but an inverse correlation to anti-neutrophil cytoplasmic antibodies during remission. Rheumatology (Oxford) 2015;54:2085-94.
15. Rudolph KL, Chang S, Lee HW, et al. Longevity, stress response, and cancer in aging telomerase-deficient mice. Cell 1999;96:701-12.
16. Yamasaki K, Schauber J, Coda A, et al. Kallikrein-mediated proteolysis regulates the antimicrobial effects of cathelicidins in skin. FASEB J 2006;20:2068-80.
17. Sangaletti S, Tripodo C, Chiodoni C, et al. Neutrophil extracellular traps mediate transfer of cytoplasmic neutrophil antigens to myeloid dendritic cells toward ANCA induction and associated autoimmunity. Blood 2012;120:3007-18.
18. Schreiber A, Rousselle A, Becker JU, et al. Necroptosis controls NET generation and mediates complement activation, endothelial damage, and autoimmune vasculitis. Proc Natl Acad Sci U S A 2017;114:E9618-25.
19. Huang YM, Wang H, Wang C, et al. Promotion of hypercoagulability in antineutrophil cytoplasmic antibody-associated vasculitis by C5a-induced tissue factor-expressing microparticles and neutrophil extracellular traps. Arthritis Rheumatol 2015;67:2780-90.
20. Kambas K, Chrysanthopoulou A, Vassilopoulos D, et al. Tissue factor expression in neutrophil extracellular traps and neutrophil derived microparticles in antineutrophil cytoplasmic antibody associated vasculitis may promote thromboinflammation and the thrombophilic state associated with the disease. Ann Rheum Dis 2014;73:1854-63.
21. Zhang D, Chen G, Manwani D, et al. Neutrophil ageing is regulated by the microbiome. Nature 2015;525:528-32.
22. Costenbader KH, Prescott J, Zee RY, et al. Immunosenescence and rheumatoid arthritis: does telomere shortening predict impending disease?

Autoimmun Rev 2011;10:569-73.

23. Coussens E, Grine L, Bostoen J, et al. Analysis of telomere length as predictive marker in psoriasis for comorbidities. Exp Dermatol 2016;25:388-90.

24. van den Hoogen LL, Sims GP, van Roon JA, et al. Aging and Systemic Lupus Erythematosus - Immunosenescence and Beyond. Curr Aging Sci 2015;8:158-77.

25. Fessler J, Raicht A, Husic R, et al. Premature senescence of T-cell subsets in axial spondyloarthritis. Ann Rheum Dis 2016;75:748-54.

26. Gounder SS, Abdullah BJJ, Radzuanb N, et al. Effect of Aging on NK Cell Population and Their Proliferation at Ex Vivo Culture Condition. Anal Cell Pathol (Amst) 2018;2018:7871814.

27. Invernizzi P, Bernuzzi F, Lleo A, et al. Telomere dysfunction in peripheral blood mononuclear cells from patients with primary biliary cirrhosis. Dig Liver Dis 2014;46:363-8.

28. Beier F, Balabanov S, Amberger CC, et al. Telomere length analysis in monocytes and lymphocytes from patients with systemic lupus erythematosus using multi-color flow-FISH. Lupus 2007;16:955-62.

29. Vogt S, Iking-Konert C, Hug F, et al. Shortening of telomeres: Evidence for replicative senescence of T cells derived from patients with Wegener's granulomatosis. Kidney Int 2003;63:2144-51.

30. Wu CH, Hsieh SC, Li KJ, et al. Premature telomere shortening in polymorphonuclear neutrophils from patients with systemic lupus erythematosus is related to the lupus disease activity. Lupus 2007;16:265-72.

31. Kordinas V, Ioannidis A, Chatzipanagiotou S. The Telomere/Telomerase System in Chronic Inflammatory Diseases. Cause or Effect? Genes (Basel) 2016. doi: 10.3390/genes7090060.

32. Tsai CY, Shen CY, Liao HT, et al. Molecular and Cellular Bases of Immunosenescence, Inflammation, and Cardiovascular Complications Mimicking "Inflammaging" in Patients with Systemic Lupus Erythematosus. Int J Mol Sci 2019. doi: 10.3390/ijms20163878.

33. Guan JZ, Guan WP, Maeda T, et al. Patients with multiple sclerosis show increased oxidative stress markers and somatic telomere length shortening. Mol Cell Biochem 2015;400:183-7.